Chapter 1

Introduction

1.1 Clusters of galaxies

Clusters of galaxies are the largest gravitationally bound structures in the universe. They have masses ranging from $\simeq$ a few $\times 10^{14} - 10^{15}\, M_{\odot}$. They typically contain tens (groups or poor clusters) to a few hundreds of galaxies (rich clusters) spread over a region of roughly $\simeq 1$ Mpc. A small fraction (about 5%) of galaxies in the present universe are bound in groups and clusters with a space density greater than one galaxy per cubic mega-parsec (about two orders of magnitude greater than the average density of galaxies in the field) (Dressler 1984). Some of these aggregations of galaxies are both dense and populous. These galaxy clusters were first studied in detail by Wolf (1906) although the tendency for galaxies to cluster on the sky had been noted long before this. A huge advance in the systematic study of the properties of clusters occurred when Abell compiled an extensive, statistically complete catalogue of rich clusters of galaxies (Abell 1958). Typically these rich clusters of galaxies contain about a few hundred galaxies with a spread in luminosity of two orders of magnitude in a volume of roughly a cubic mega parsec or more. Compared to these clusters, poor clusters or groups contain few tens of galaxies with relatively high space densities compared to the average density of galaxies in the field (Bahcall 1980). Optical photographs of two of the several most studied clusters of galaxies are shown in Figure (1.1). The Virgo cluster is the nearest rich cluster to our own galaxy (Figure (1.1a)); the Coma cluster is the nearest cluster (Figure (1.1b)). Galaxies in clusters are mostly of the early type, i.e. elliptical or S0 galaxies, than late-type galaxies like spirals or irregulars. Rich clusters often contain a centrally dominant galaxy (Mathews et al. 1964), typically a giant elliptical or S0, known as the cD galaxy. Such galaxies normally reside in the deepest part of the potential well (Oegerle & Hill 1994) and are at the peak of the cluster X-ray emission (Jones et al. 1979). Historically, clusters were first catalogued in the optical waveband. The two most extensive and often cited catalogues of rich clusters of galaxies are those of Abell (1958) and Zwicky and his collaborators (Zwicky et al. 1961-1968). Both these catalogues were constructed by identifying clusters as enhancements in the surface number density of galaxies on the National Geographic Society - Palomar Observatory Sky Survey (Minkowski & Abell 1963). A number of smaller catalogues have also now been compiled, consisting of clusters in the southern sky or clusters at higher redshifts ($z \lesssim 0.2$).

1.1.1 The intracluster medium

In 1966, X-ray emission was detected outside our galaxy for the first time. This was from the region around the galaxy M87 in the centre of the Virgo cluster (Byram et al. 1966; Bradt et al. 1967). Five years later, X-ray sources were also detected in the directions of the Coma and Perseus clusters (Fritz et al. 1971; Gursky et al. 1971a, b; Meekins et al. 1971). Since these are three of the nearest rich clusters, it was suggested that clusters of galaxies might generally be X-ray sources (Cavaliere et al. 1971). The launch of the *Uhuru* X-ray astronomy satellite permitted a survey of the entire sky for X-ray emission (Giacconi et al. 1972) and established that this was indeed the case. These early *Uhuru* observations indicated that clusters were bright X-ray sources, with luminosities typically in the range of 10^{44} erg s^{-1}. These X-ray sources associated with clusters were found to be spatially extended; their sizes being comparable to the size of the galaxy distribution in the clusters (Kellogg et al. 1972; Forman et al. 1972). Unlike other bright X-ray sources, cluster X-ray sources did not vary temporally in their brightness (Elvis 1976). Although several emission mechanisms like inverse

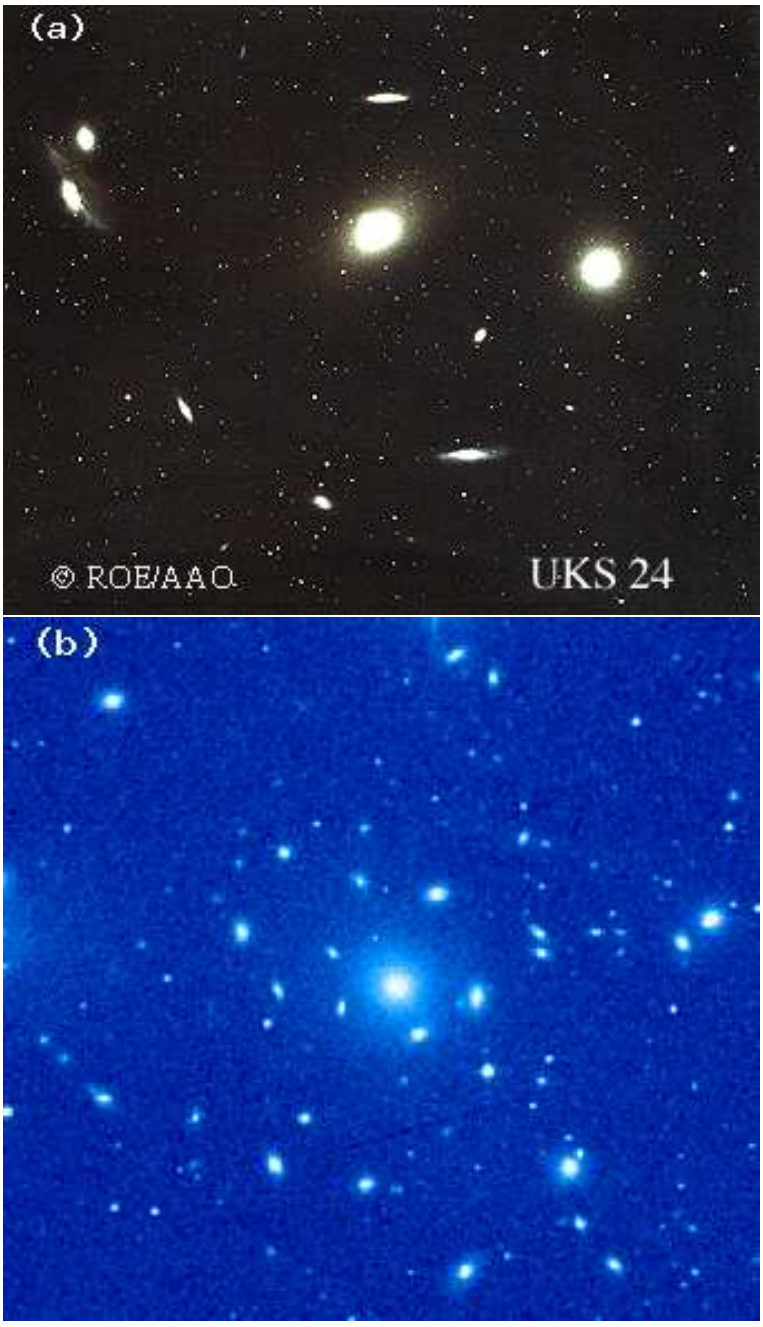

Figure 1.1: Optical photographs of clusters of galaxies. (a) An optical photograph of the Virgo cluster of galaxies. Pictured are several galaxies of the Virgo Cluster, the closest cluster of galaxies to the Milky Way. The Virgo Cluster spans more than 5 degrees on the sky - about 10 times the angle made by a full Moon. It contains over 100 galaxies of many types - including spirals, ellipticals, and irregular galaxies. The Virgo Cluster is so massive that it is noticeably pulling our Galaxy toward it. The above picture includes two galaxies that are also Messier objects: M84 and M86. M84 is the bright elliptical galaxy just above the center of the photograph, and M86 is the bright elliptical galaxy to its right. Photograph taken from APOD. (b) The Coma Cluster of galaxies pictured is a dense cluster containing many thousands of galaxies. This picture was created at the WWW site Skyview, a "virtual observatory" where it is possible to view any part of the sky in wavelengths from radio to gamma-ray. Photograph taken from APOD.

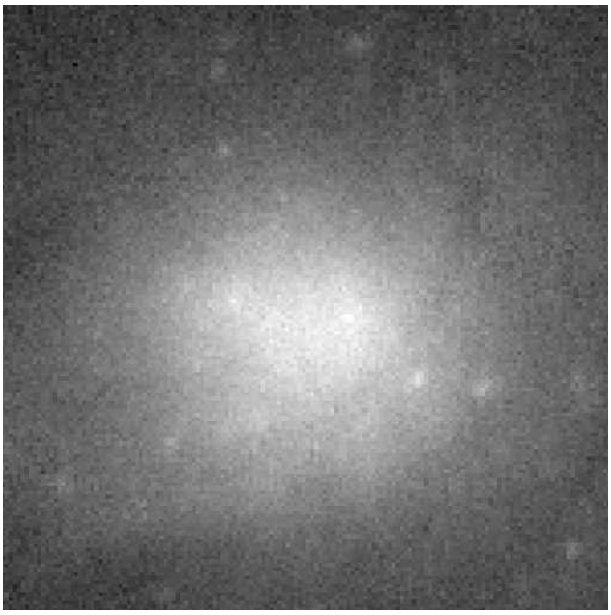

Figure 1.2: X-ray image of the central 1 Mpc of Coma cluster. The image was taken from `http://spiff.rit.edu/classes/phys240/lectures/gal_cluster/gal_cluster.html` of Michael Richmond's lectures.

Compton emission of cosmic microwave background photons up to X-ray energies by relativistic electrons within the cluster (Brecher & Burbridge 1972; Bridle & Feldman 1972; Costain et al. 1972; Perola & Reinhardt 1972; Harris & Romanishin 1974; Rephaeli 1977a, b) or emission due to a population of individual X-ray sources, like those found in our galaxy (Katz 1976; Fabian et al. 1976) were proposed, the X-ray spectra of clusters were most consistent with thermal bremsstrahlung from hot gas (Felten et al. 1966).

This interpretation required that the space in between the galaxies in clusters be filled with very hot ($\simeq 10^8$ K), low density ($\simeq 10^{-3}$ atoms/cm^3) gas. At such temperatures and densities, the primary emission for a gas composed mainly of hydrogen is thermal bremsstrahlung (free-free) emission. The bremsstrahlung emissivity at a frequency ν of a plasma with ions of charge Z and an electron temperature T_e is given by

$$\epsilon_\nu^{ff} = \frac{2^5\pi e^6}{3m_e c^2}\left(\frac{2\pi}{3m_e k_b}\right)^{1/2} Z^2 n_e n_i g_{ff}(Z, T_e, \nu) \times T_e^{-1/2}\exp(-h\nu/k_b T_e) \qquad (1.1)$$

where n_i and n_e are the number density of ions and electrons, respectively. The Gaunt factor $g_{ff}(Z, T_e, \nu)$ corrects for quantum mechanical effects and for the effect of distant collisions, and is slowly varying function of frequency and temperature, as given in Karzas & Latter (1961) and Kellogg et al. (1975). In fact, the observed X-ray spectra are generally fit fairly well by equation (1.1), with gas temperatures of 2×10^7 to 10^8 K, with the emission falling off rapidly at high frequencies, as is observed (see review on X-ray emission from clusters by Sarazin, 1988). The clearest evidence in favour of the thermal bremsstrahlung model was the detection of strong X-ray line emission from clusters. In 1976, X-ray line emission from iron (Fe) was detected from the Perseus cluster of galaxies (Mitchell et al. 1976), and shortly thereafter from Coma and Virgo as well (Serlemitsos et al. 1977). The emission mechanism for this strong 7 keV line was deduced to be thermal since this emission

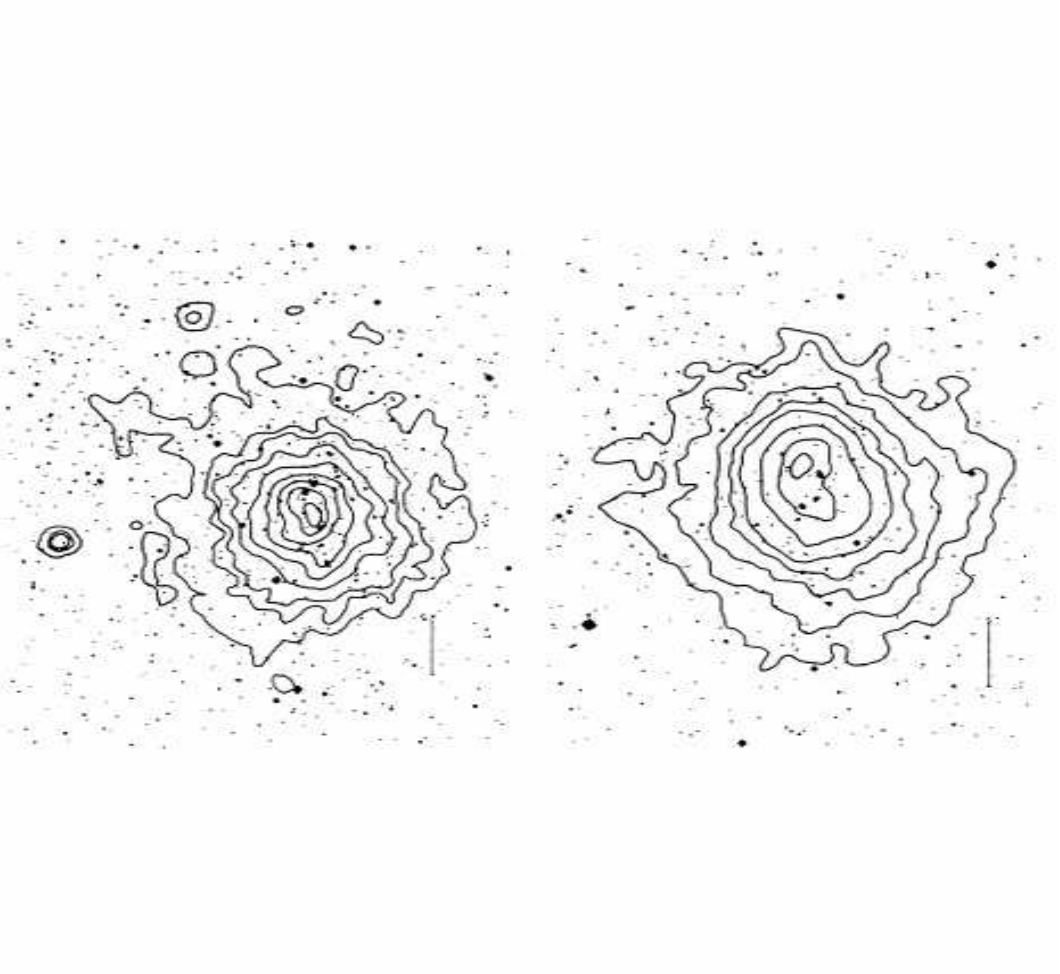

Figure 1.3: X-ray isointensity of A2255 (left) and A2256 (right) superposed on optical photographs. The smooth and symmetrical X-ray intensity distribution shows that these clusters are relaxed and virialized. Images taken from Jones & Forman (1982).

could be naturally reconciled with the ICM model with solar abundances of heavy elements. Thus, its detection confirmed the thermal interpretation of cluster X-ray sources (see review by Sarazin 1988).

It is now confirmed that the bulk of baryonic matter in clusters consists of X-ray emitting plasma at temperatures of tens of million Kelvin and is known as the intracluster gas (ICM). The majority of the X-ray emission from the cluster comes from the ICM, and typically is in the range from 10^{42} to about 10^{45} erg s^{-1} (Forman & Jones, 1982). Figure (1.2) shows the X-ray image of the central 1 Mpc of the Coma cluster. The X-ray emission is seen to be mostly diffuse and spread over the entire region and not just concentrated in regions where the cluster galaxies are located. The ICM has densities of 10^{-4} to 10^{-2} cm^{-3} and temperatures of 2×10^{7}–10^{8} K. The total mass of the gas is of the order of few$\times10^{13}$ to $10^{14}\,M_{\odot}$. As to the origin of this gas, it is widely assumed that it had simply fallen into the clusters from the great volumes of space between them, where it had been stored since the formation of the universe (Gunn & Gott, 1972).

1.1.2 Dark matter in galaxy clusters and the intracluster medium

In the Cold Dark Matter (CDM) paradigm set out by Peebles 1982, Blumenthal et al. 1984 and Davis et al. 1985, galaxy clusters arise from the gravitational collapse of rare high peaks of primordial density perturbations in the hierarchical clustering scenario for the formation of cosmic structures (Kaiser 1984; Bardeen et al. 1986; see Peebles 1980; Coles & Luchin 1995; Peacock 1999 for details). It assumes that the matter content of the universe is dominated by an unidentified weakly interacting massive particle called the dark matter, whose gravitational effects are responsible for the dynamics of both galaxies and clusters. In this cosmogony, structures like galaxies and clusters are known to form through non-linear gravitational collapse of dark matter, involving both periods of steady accretion of mass, as well as violent merging episodes, in which two haloes of comparable mass collide to give birth to a larger halo. Galaxy clusters form from such collapse of cosmic matter over a region of several mega-parsecs. Cosmic baryons, which represent approximately 15% of the mass content of the universe, follow the dynamically dominant dark matter during the collapse and are trapped within these gravitational potential wells created by the dark matter haloes. At galaxy scales, they condense and cool within these dark matter haloes (Rees & Ostriker 1977; White & Rees 1978) and thus illuminate these structures. However in galaxy clusters, baryons are found in a hot, diffuse, ionized plasma that constitutes the intracluster medium (ICM) (discussed in the earlier section).

The first evidence for the presence of dark matter in clusters was noticed by Smith (1936). In his study of the Virgo cluster, he found that the mass implied by cluster galaxy motions largely exceeded that associated with the optical light component. This was confirmed next by Zwicky (1937). Dynamical measures of the quantity of mass in clusters rely on the basic Newtonian relation $M\,(<r) \approx \upsilon^2 r/G$. One assumes that the system is virialized or relaxed and incorporates various possibilities for likely anisotropies in the galaxy orbits. This method is fundamentally limited by the statistics of the finite number of galaxies as well as ambiguities about the cluster membership (Canizares, 1999).

The crossing time for a cluster of size $R_{\rm cl}$ can be defined as

$$t_{\rm cr} = \frac{R_{\rm cl}}{\sigma_{\rm v}} \simeq 1\left(\frac{R_{\rm cl}}{1{\rm Mpc}}\right)\left(\frac{\sigma_{\rm v}}{10^3\,{\rm km\,s^{-1}}}\right)^{-1}{\rm Gyr}\,. \tag{1.2}$$

Therefore, in a Hubble time, $t_H \simeq 10$ Gyr, such a system has enough time in its internal region, $\lesssim 1\,h^{-1}$Mpc, to dynamically relax – a condition that cannot be attained in the surrounding, ~ 10 Mpc, environment. Assuming virial equilibrium, the typical cluster mass is

$$M_{\rm cl} \simeq \frac{R_{\rm cl}\sigma_{\rm v}^2}{G} \simeq \left(\frac{R_{\rm cl}}{1\,h^{-1}{\rm Mpc}}\right)\left(\frac{\sigma_{\rm v}}{10^3\,{\rm km\,s^{-1}}}\right)^2 10^{15}\,h^{-1}M_\odot\,. \tag{1.3}$$

Now, $\sigma_{\rm v}$ and $R_{\rm cl}$ can be evaluated from the radial velocity distribution and the projected spatial distribution of a fair sample of galaxies if one assumes that the positions of galaxies and the orientation of their velocity vectors are uncorrelated (Limber & Mathews 1960). The first observations showed that clusters of galaxies are associated with deep gravitational potential wells, containing galaxies with a typical velocity dispersion along the line-of-sight of $\sigma_{\rm v} \simeq 10^3$ km s^{-1} and $R_{\rm cl} \simeq 1$ Mpc typically. Thus for a region of $1\,h^{-1}$Mpc (which would have relaxed within a Hubble time) with $\sigma_{\rm v} \simeq 10^3$ km s^{-1} (average rich cluster parameters), the total mass enclosed is $M_{\rm cl} \simeq 10^{15}\,{\rm M}_\odot$ typically.

Another method which is extensively used to determine the total gravitational mass of clusters and thus conclude about their dark matter content is X-ray observations. The test particles, here, are electrons in the diffuse, hot plasma whose velocity is determined by measuring the plasma temperature which is typically around 10^8 K. In this method there are no velocity anisotropies to be dealt with because the plasma is a collisional gas, but it is necessary to assume hydrostatic equilibrium, an assumption made plausible by the very regular, nearly circular X-ray images of many clusters (Forman & Jones, 1982; Jones & Forman, 1984). This can be seen from Figure (1.3) where the X-ray surface brightness contours of both clusters, A2255 and A2256 are circular.

One example of the few clusters for which a full, joint analysis of optical and X-ray data has been performed is A2256 (Henry et al. 1993 and Fabricant et al. 1989) with the ROSAT observatory. The derived total mass density for A2256, and the visible components in gas or galaxies, are shown in Figure (1.4). For A2256, Henry et al. (1993) found a total binding mass of $0.5 \pm 0.1 \times 10^{15}{\rm M}_\odot$ within $0.76\,h_{100}^2$ Mpc.

Thus it can be concluded that there is abundant evidence from dynamical studies that clusters with a wide range of richness contain significant amounts of dark matter. Recently, evidence for significant quantities of dark matter has also been found in poor groups (Mulchaey et al., 1993; Ponman & Bertram 1993; Ponman et al. 1994; Henriksen & Mammon 1994; see review by Mulchaey 2000; Helsdon & Ponman 2003). The X-ray data have traditionally been fit by models with a core radius, within which the dark matter density profile becomes constant; with $\rho_{\rm dm}(r) \propto r^{-2}$ and $\propto r^{-3}$ at larger radii. Typical core radii are around 100 to 400 kpc.

Another important tool to infer the total gravitational mass content in clusters is gravitational lensing (Pello et al. 1991; Schneider et al. 1992; Kayser et al. 1992; Fort & Mellier 1994; and references therein). Clusters and the galaxies they contain are very effective gravitational lenses, which both magnify and distort the images of distant galaxies seen through the cluster. The strongest portion of the lens is generally through the central 10–20 arc sec of the cluster. In the "thin lens" approximation, appropriate for clusters, the strength of the lens is related to the surface mass density projected on the sky. To get strong lensing, required for the so-called giant arcs, the surface mass density must be $\geq \Sigma_{\rm crit}$, which has the surprisingly terrestrial value of $\approx 0.5 - 1.0$ g cm^{-2}. For reference, this is comparable to a few times the closure density (corresponding to $\Omega = 1$ projected over the Hubble distance $D_{\rm H_0} = c/H_0$) ie. $\rho_{\rm c} \times D_{\rm H_0} \simeq 0.12$ g cm^{-2}.

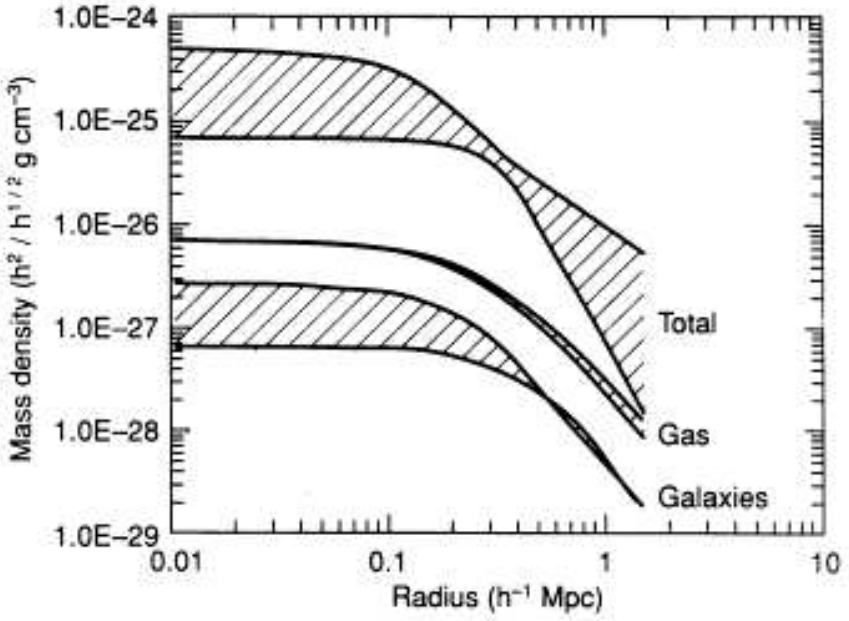

Figure 1.4: The total, hot gas and galaxy densities as a function of radius in A2256 as determined from the X-ray analysis of Henry et al. 1993. The width of the band gives an estimate of the 68% confidence ranges.

Expressed in terms of mass enclosed within the radius of the arc, one has

$$M(R_{\rm arc}) \approx \frac{c^2 R_{\rm arc}}{4G}\left(\frac{R_{\rm arc}}{D_{\rm H_o}}\right)\left(\frac{D_{\rm OS}}{D_{\rm OL}D_{\rm LS}}\right) \tag{1.4}$$

where $D_{\rm OS}$, $D_{\rm OL}$ and $D_{\rm LS}$ are the angular diameter distances from observer to source, observer to lens and lens to source respectively.

With the refurbishment of the HST, spectacular images of arc(let)s and multiply imaged galaxies have permitted enormous progress in this field. It turns out that giant arcs are no longer the strongest constraints on cluster mass distribution, because similar and even better information can be obtained with spatially resolved HST images of arc-lets. The usual mass reconstruction technique using arc(let)s present in the innermost regions (close to the critical lines where arcs are located) is based on the assumption that the cluster mass density is smoothly distributed and can be expressed analytically, possibly with addition of some substructures, and on the hypothesis that the observed arc(let)s correspond to rather generic lens configurations, like caustics. These assumptions have already provided some convincing results using ground-based images, in particular with predictions of the position of additional images (counter images) associated with arc(let)s (Hammer & Rigaud 1989; Mellier et al. 1993; Kneib et al 1993, 1995). In all cases, it was found that the core radius of the dark matter distribution is small ($< 50h_{100}^{-1}$ kpc) and that its geometry is compatible with the faint extended envelopes of light surrounding the giant cluster galaxies. The new investigations using the detailed morphology of the numerous arc(let)s visible in the HST images have provided more refined constraints on the dark matter distribution on the 100 kpc-scale (Hammer et al 1997, Gioia et al 1998, Kneib el al 1996, Tyson et al 1998). They confirm the trends inferred from previous ground-based data (see review by Mellier 1999 for details).

Another powerful and complementary way to recover the mass distribution of clusters of galaxies had been proposed by Kaiser & Squires (1993). It is based on the distribution of weakly lensed galaxies rather than the use of giant arcs. In 1988, Fort et al. (1988) obtained at CFHT deep sub-arcsecond images of the lensing-cluster A370 and observed the first weakly distorted galaxies ever detected. The galaxy number density of their observation was about 30 arc-min^{-2}, mostly composed of background sources, far beyond the cluster. These galaxies lensed by the cluster show a correlated distribution of ellipticity/orientation which maps the projected mass density. The first attempt to use this distribution of arc-lets as a probe of dark matter was undertaken by Tyson et al. (1990). The first cluster mass reconstructions using the Kaiser & Squires linear inversion was done by Smail (1993) and Fahlman et al (1994). This technique, which has been further developed in recent times, can actually find mass distributions in much larger distance scales ($\approx$1 Mpc) in clusters, as compared to the strong lensing technique which only can find mass distribution within the cluster cores.

Although relatively few arc systems have been modeled in detail, there is at least qualitative agreement between the strong lensing models and the dynamical results from both X-ray and optical (Fort & Mellier 1994; Miralda-Escude 1995). Weak lensing studies of several clusters also show that on scales of about 1 Mpc, the geometry of mass distributions, the X-ray distribution and the galaxy distribution are similar, though the ratio of each component with respect to the others may vary with radius (see review of Mellier 1999). Thus it can be concluded that 80-90% of the total mass in clusters, both rich and poor, is dark. Both the visible galaxies and the X-ray emitting gas correlate with the dark matter and follow it but neither is an exact tracer. There are also processes other than gravitational interactions which occur in the baryonic medium (ICM) in clusters and have considerable effects on their physical properties. However to conclude, it can be said that the dynamics of galaxies and ICM and their physical states are mostly determined by the dark matter content in galaxy clusters.

1.2 The self-similar hierarchical picture and baryons

An important constraint on theories of formation of cosmological structures is that they should be able to account for the properties of rich clusters of galaxies. Ignoring the gas content, high resolution *N*-body techniques are used to simulate the gravitational collapse of clusters and to study their mass content and profiles. From the theoretical point of view, there are simple models which can predict the growth of non-linear structures by gravitational instability from general linear scale-free initial conditions. The basic problem of the collisionless collapse of a spherical perturbation in an expanding background was first addressed by Gunn & Gott (1972) and Gunn (1977), where the cosmological expansion and the role of adiabatic invariance were first introduced in the context of formation of individual objects. The next step was achieved by Fillmore & Goldreich (1984) and Bertschinger (1985) when they found analytical predictions for the density of collapsed objects seeded by scale-free primordial perturbations in a flat universe.

1.2.1 Spherical collapse

One of the simplest models for the growth of non-linear structures by gravitational instability is provided by the homogeneous spherical collapse model. In this model, a spherical region with homoge-

neous constant density is replaced with a somewhat smaller concentric sphere of matter. This makes the sphere slightly over-dense as compared to the outer regions. The age of this "pressure-less dust" sphere is so arranged that it is same as that of the background Universe, but that this sphere has negative total energy. Thus at an initial time $t_{\rm i}$, the density perturbation (averaged over the whole sphere) has an amplitude $\delta_{\rm i} = (\rho_{\rm i}(r) - \overline{\rho})/\overline{\rho} > 0$ and $|\delta_{\rm i}| \ll 1$. This sphere is taken to be expanding with the background universe in such a way that the initial peculiar velocity at the edge, $V_{\rm i}$ is zero. The time evolution of such an inhomogeneity is studied in this model (Appendix A). For an Einstein-de Sitter universe, the maximum radius at turn around (i.e. where this sphere of matter would stop expanding with the background universe and start its collapse), $r_{\rm m}$ and the *turn-around* time, $t_{\rm m}$, can be analytically solved for a given initial perturbation, δ_i. This model predicts that the average density contrast of collapsed structures at any particular epoch, z, are same and is a function of the background density, $\rho_{\rm b}$ ie. a constant at any given epoch. For an Einstein-de Sitter universe, the non-linear density contrast of a collapsed structure $\simeq 180$ and its linear extrapolation is $\simeq 1.68$. Thus

$$\begin{aligned} \rho_{\rm dm,c} &\simeq \Delta_{\rm c}(z)\rho_{\rm b}(z) \\ &\simeq 180\rho_{\rm b}(z) \quad \text{(for Einstein} - \text{de Sitter universe)}, \end{aligned} \tag{1.5}$$

where, $\Delta_{\rm c}(z)$ is the critical over-density at the time of collapse for any cosmological model.

In principle, the reasons for which the spherical collapse picture should be able to predict the density distribution of dark matter haloes is not clear. This is because the assembly of structures in the universe is not expected to proceed by the infall of spherical shells, but rather through a hierarchical series of merging events. Nonetheless, this model of spherical infall is very useful in describing the non-linear regime in structure formation. It seems to reproduce features like the average density distribution which have been seen in full scale numerical simulations of dark matter haloes (Zaroubi 1996; Moore et al. 1999; Łokas & Hoffman 2000; Ascasibar et al. 2004) and makes predictions about different properties of rich clusters like X-ray luminosity, gas mass profiles which match roughly with observations (Kaiser 1986).

1.2.2 Self-similar hierarchical evolution

In the hierarchical picture of structure formation, cosmic structure grows via gravitational instabilities from small perturbations seeded in an early inflationary epoch. Since most of the mass is in the form of collisionless cold dark matter, this dark matter determines the dynamics of baryons on large scales, where hydrodynamic forces are unimportant compared to gravity.

In this picture, the initial small-amplitude density perturbations are assumed to take the form of some homogeneous and isotropic random process. This initial density field gives rise to a hierarchy of collapsing structures as the power spectrum for ΛCDM universe is such where smaller mass structures collapse first. While the linear growth of fluctuations of arbitrary form can be solved analytically, the situation becomes very complicated when the fluctuations turn around and collapse. However simulations show us that at any time, concentrations of masses ie. collapsed structures progressively come together and merge into larger bound structures (e.g. Frenk et al. 1988, Peebles 1993, Coles & Lucchin 2002, Padmanabhan 1993 and references therein).

In the linear evolution of perturbations, there is a special set of initial conditions which are scale-free. These initial conditions come from a background universe which has $\Omega_{\rm tot} = \Omega_{\rm m} + \Omega_\Lambda = 1$

(a scale is introduced in the background universe when it is open or closed which is the scale of curvature). So the amplitude of the initial density fluctuations is a power-law function and thus scale-free. However, this initial self-similar spectrum gets modified as the universe evolves and the fluctuations enter the horizon at the epoch of matter-radiation equality, $z_{\rm eq}$, and it typically picks this scale. On scales corresponding to rich clusters, this scale is not important since they lie in a narrow range of masses and the spectral index of the density fluctuations essentially remain a constant.

In addition, there is yet another scale which these initial self-similar spectrum of fluctuations pick as they further evolve into the non-linear regime. In this regime, the density perturbations pick the important physical scale in the problem, the mass-or-length scale of those fluctuations which are going non-linear, $M_{\rm NL}$. Thus any dimensionless statistical property of the final density perturbations become only a function of $M/M_{\rm NL}$ and thus the final state ie. the average density contrast of a collapsed structure is temporally self-similar. This approximation of self-similarity is valid and reasonable for rich clusters since in these narrow range of masses, even in non-linear regime, the coupling between fluctuations on very different mass scales is very weak. However, this assumption might pose a problem if we go down in mass to very poor clusters and groups. To conclude, we can say that for clusters, it is reasonable to model them as scaled versions of one another having dark matter densities as universal.

1.2.3 Universal density profile of dark matter

One of the most interesting properties of the dark matter haloes found in numerical simulations is the apparent universality of their radial density profiles, valid over several orders of magnitude in mass.

Early numerical work of Quinn et al. (1986) and Frenk et al. (1988), showed that dark matter haloes have an isothermal structure (i.e. $\rho_{\rm dm} \propto r^{-2}$). However, later high resolution simulations by Dubinski & Carlberg (1991) and Crone et al. (1994) had enough resolution to detect the first evidence of non-power-law density profiles. Following these, Navarro et al. (1996, 1997, hereafter NFW) found that haloes in their numerical simulations could be fitted by a simple analytical function with only two parameters (e.g. a characteristic density and a characteristic radius). Their main result was that the radial density profile was steeper than isothermal ($\rho_{\rm dm} \propto r^{-3}$) for large radii, and shallower (but still diverging as $\rho_{\rm dm} \propto r^{-1}$) near the centre. The corresponding logarithmic slope

$$\alpha(r) \equiv \frac{d \log \rho_{\rm dm}(r)}{d \log r} \tag{1.6}$$

varied smoothly between these two extreme values, being equal to isothermal ($\alpha = -2$) at the characteristic radius only.

Navarro et al. (1997) further showed that the characteristic parameters of a dark matter halo seem to correlate to a certain extent. If this is true, then the final mass distribution of objects of different mass could be described in terms of one-parameter family of analytical profiles. This also implies that the many relevant quantities, such as virial mass, central density, or formation time, must be correlated. Similar results have been found in several independent studies, using much higher mass and force resolution than the original NFW. However, there is still some disagreement about the innermost value of the logarithmic slope α and its dependence on resolution. Moore et al. (1998a, 1999b), Ghinga et al. (1998, 2000) and Fukushige & Makino (1997, 2001, 2003) find even steeper

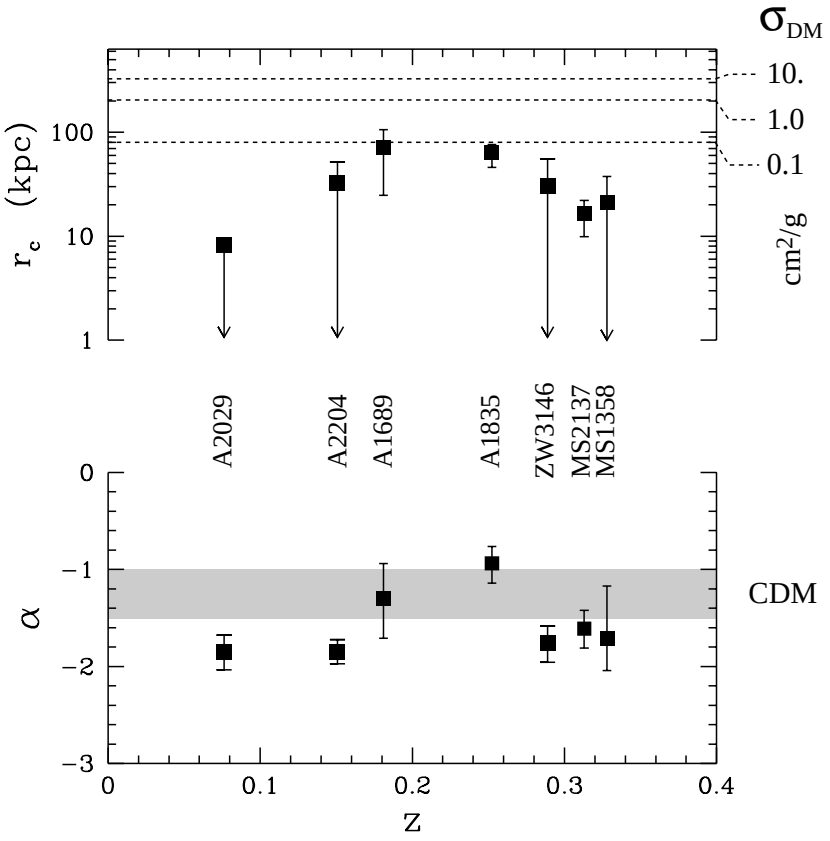

Figure 1.5: Results from a spectroscopic de-projection analysis of a sample of 10 relaxed galaxy clusters by Arabadjis et al. 2004 (astro-ph/0408362). A summary of the softened isothermal sphere core radii (top) and power law slopes (bottom) are shown here. The gray band denotes the inner slope predictions of numerical CDM experiments bracketed by the values from Navarro et al. (1996, 1997) at α = -1 and Moore et al. (1996) at α = -1.5

density profiles near the centre ($\alpha = -1.5$), whereas other authors (Jing & Suto 2000; Klypin et al. 2001) claim that the actual value of α may depend on halo mass, merger history and substructure.

Observationally, the cold dark matter scenario, originally proposed to explain the observed flat rotation curves of spiral galaxies, is extremely successful in describing the large-scale structure of the universe and even the whole process of structure formation. Observations have shown an agreement with the NFW profile for rich clusters, though there are problems with the universality of the value of α at lower masses e.g. in dwarf spiral and LSB galaxies (Flores & Primack 1994; Marchesini et al. 2002 and so on). Figure (1.5) shows the results from a deprojection analysis of a sample of 10 relaxed galaxy clusters taken from Arabadjis et al. (2004) (astro-ph/0408362). This figure shows a summary of the softened isothermal core radii (top) and the power law slopes (bottom) of the softened NFW profile. The gray band in the figure denotes the inner slope predictions of numerical CDM experiments bracketed by the values from Navarro et al. (1996, 1997) at $\alpha = -1$ and Moore et al. (1996) at $\alpha = -1.5$. As we see here, there is a fair agreement of the logarithmic slopes determined from the X-ray observations of this sample of clusters with the NFW values. They find that the central density slopes are mostly consistent with the predictions of Λ-CDM: $-1 \lesssim \alpha \lesssim -2$. They use a smoothed NFW profile with a core radius, r_c and also constrain the core size of the clusters. Recent lensing observations also point to the fact that there might be a core in the dark matter profile in clusters of the order of $\sim$ tens of kilo-parsecs (Tyson et al., 1998; Shapiro & Iliev, 2000). Thus a NFW profile with a softened core might be a better representation of dark matter profile and their universal behaviour in clusters.

All this leads us to the question as to how would the baryons which are trapped in these dark matter potential wells behave? Is it possible to predict the behaviour of the baryonic gas and their observed properties from these known scaling laws of the gravitationally dominant dark matter in galaxy clusters?

1.2.4 Gas infall and virialization in clusters

In the discussion so far on galaxy clusters and their formation, we have only considered collisionless particles and their dynamics due to gravity. However, observable properties of the intracluster medium (in X-rays) are determined by the physical state and the spatial distribution of the baryonic component in the form of diffuse intracluster medium. So, it is extremely important to connect these theories of structure formation to the baryons inside galaxy clusters to be able to predict their properties, either by resorting to phenomenological relations between the dark and luminous components or by direct self-consistent numerical modelling.

In principle, hot gas in clusters of galaxies should be easy to understand. Because of the relatively low ratio of baryons to dark matter, the potential of a cluster is dark matter dominated. The dynamical time within a cluster is shorter than a Hubble time, so most clusters should be relaxed (see below). Also, the cooling time of most of the intracluster gas is longer than a Hubble time except that lying in the very central regions of clusters. The same will be true of the somewhat smaller units from which these clusters have assembled in the hierarchical scenario. The temperature of these sub-units will be typically lower than the virial temperature of the final cluster. Thus the infall/merging process of these sub-units will be supersonic, and the gas will be heated to the virial temperature by shocking. This

process will be tremendously complicated. If dissipation is neglected, no additional physical scale is introduced in this process. As a result the scaling laws of the collisionless dark matter component will apply to this adiabatic gas component also. This would mean that the global properties of clusters, such as halo mass, emission-weighted temperature, X-ray luminosity and entropy would scale self-similarly (Kaiser 1986). This would also imply that the mean gas density ($\rho_{\rm gas}$) would follow the mean dark matter density ($\rho_{\rm dm}$) of the collapsed structure. Thus,

$$\rho_{\rm gas}\ \text{(for a collapsed cluster)} \simeq const.\ \text{(at a particular epoch)} \tag{1.7}$$

Even, numerical simulations that include adiabatic gas-dynamics produce clusters of galaxies that obey these scaling laws (e.g. Evrard et al. 1996; Bryan & Norman 1998).

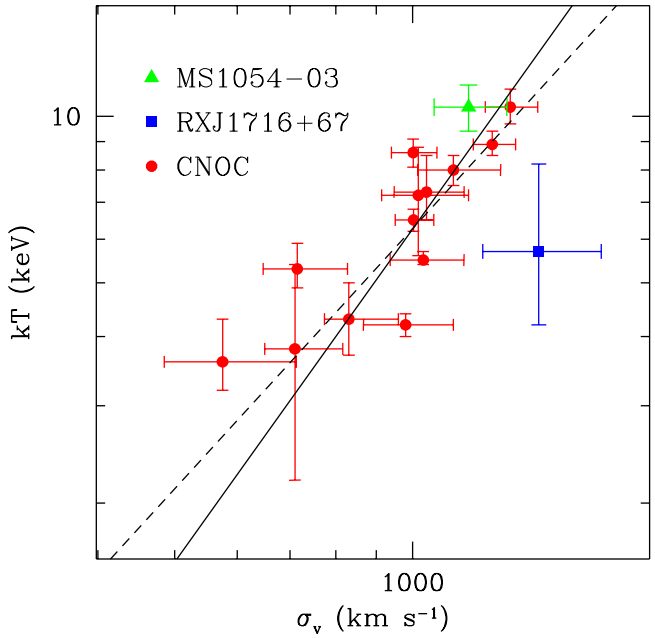

Figure 1.6: The relation between velocity dispersion, σ_v, and ICM temperature, T, for distant ($z > 0.15$) galaxy clusters. The solid line shows the relation $k_{\rm b}T_{\rm gas} = \mu m_p \sigma_v^2$, and the dashed line is the best–fit to the low–z T–σ_v relation from Wu et al. (1999). The figure has been taken from Rosati et al. 2002.

Observations of galaxy clusters in the X-ray band have revealed that the intracluster medium is hot and of temperatures of the order of $\simeq$ a few times 10^7 to 10^8 K. The gas, the member galaxies and the dark matter are mostly believed to be in virial equilibrium with each other and thus they all share the same dynamics. Thus the thermal velocity of protons in the ICM, $v_{\rm th,\,proton} \simeq \sigma_{\rm v}$, the velocity dispersion of galaxies. As a result, the temperature of the ICM ($T_{\rm gas}$) is determined also by the depth of the gravitational potential well it is residing in. It is typically given by

$$k_{\rm b}T_{\rm gas} \simeq \mu m_{\rm p} v_{\rm th,proton}^2 \simeq 6\left(\frac{\sigma_{\rm v}}{10^3\ {\rm kms}^{-1}}\right)^2\ {\rm keV} \simeq \frac{GM_{\rm cl}}{R_{\rm cl}}, \tag{1.8}$$

where m_p is the proton mass and μ is the mean molecular weight (μ=0.6 for a primordial composition with a 76% fraction contributed by hydrogen). Observational data for nearby clusters (Wu et al. 1999) and for distant clusters are actually seen to follow this relation (Figure (1.6)), although with some scatter (Rosati et al. 2002). This correlation indicates that the idealized picture of clusters as relaxed structures in which both gas and galaxies feel the same dynamics is a reasonable representation. There are exceptions though which reveal the presence of more complex processes influencing the dynamics of the baryonic gas in clusters.

1.2.5 Observable properties of the ICM

Let us now take a look at the other observable properties of the intracluster medium like X-ray luminosity, density profiles, gas entropy to see if they satisfy the predicted scaling relations.

1.2.5.1 X-ray luminosity

A scaling law that is directly observable is the correlation between bolometric X-ray luminosity and gas temperature, $T_{\rm gas}$. It is known that bremsstrahlung emissivity is given by (using self-similarity)

$$\begin{aligned} L_{\rm X} &\propto n_{\rm e}\, n_{\rm i}\, T_{\rm gas}^{1/2}\, R_{\rm cl}^3 \propto \rho_{\rm gas}^2\, T_{\rm gas}^{1/2}\, R_{\rm cl}^3 \\ &\propto T_{\rm gas}^2 \end{aligned} \tag{1.9}$$

where, $n_{\rm e}$ is the electron number density and $n_{\rm i}$ is the ion density and since $T_{\rm gas} \propto (GM_{\rm cl}/R_{\rm cl}) \propto R_{\rm cl}^2$ as the mean density, $\rho_{\rm gas} = const.$ at any particular epoch (Equation (1.7)). Thus $L_{\rm X} \propto T_{\rm gas}^2$ or equivalently $L_{\rm X} \propto M_{\rm cl}^{4/3}$ at any particular epoch, z.

However, the observed $L_{\rm X}$–$T_{\rm gas}$ relation shows that the above scaling is not satisfied. In fact, the $L_{\rm X}$–$T_{\rm gas}$ relation is far steeper than the self-similar predictions. The observed relation is $L_{\rm X} \propto T_{\rm gas}^3$ (e.g. Mitchell et al. 1979; Edge & Stewart 1991; David et al. 1993; Fabian 1994) for $T_{\rm gas} \gtrsim 2$ keV and possibly even steeper for $T_{\rm gas} \lesssim 1$ keV groups. This result is consistent with the finding that $L_{\rm X} \propto M_{\rm cl}^{\alpha}$ with $\alpha \simeq {}^{1.8\pm0.1}$ for the observed mass-luminosity relation (e.g. Reiprich & Böhringer 2002). Thus observations of X-ray luminosity versus temperature of clusters and groups find that there is considerable deviation from the self-similar scalings.

1.2.5.2 Density profile of gas

A popular description of the gas density profile is the so-called β-model,

$$\rho_{\rm gas}(r) = \rho_0 \left[1 + \left(\frac{r}{r_{\rm c}}\right)^2\right]^{-3\beta/2} \tag{1.10}$$

introduced by Cavaliere & Fusco-Femiano (1976; see also Sarazin 1988 and references therein) to describe an isothermal gas in hydrostatic equilibrium with a dark matter potential that follows an analytical King profile (King 1962), $\rho_{\rm dm}(r) \propto 1/(1+x^2)^{3/2}$ where $x \equiv r/r_{\rm c}$, $r_{\rm c}$ being the core-radius. This β-profile was introduced to describe the X-ray surface brightness profiles of galaxy clusters. This parameter β is the ratio between kinetic dark matter energy and thermal gas energy (see Equation (1.8)). This form for the density profile has been widely used in the literature (see e.g. Rosati et al. 2002, for a review).

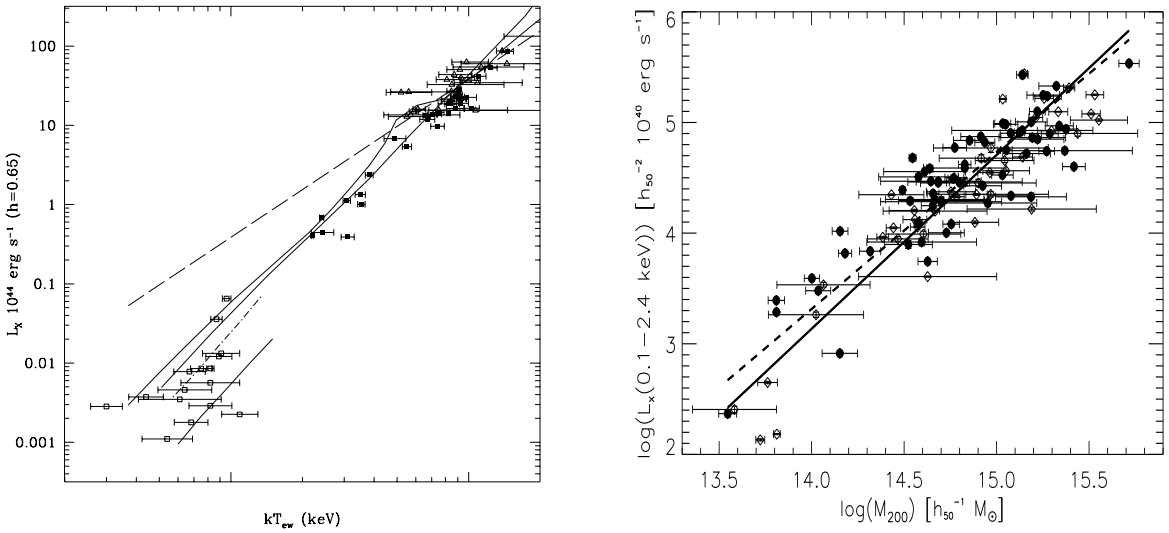

Figure 1.7: (*Left*): Relation between bolometric luminosity and emission-weighted temperature in Λ-CDM. Data are from Arnaud & Evrard (1999; filled squares), Allen & Fabian (1998; empty triangles), and Ponman et al. (1996; empty squares). The dashed line refers to the self-similar case. The thick and thin sold lines refer to different pre-heated models of cluster formation. The lower thick solid line for $T_{\rm gas} \leq 1.5$ keV shows the L-T relation at z = 0 defined within the projected radius of 100 h^{-1} kpc as in Ponman et al. (1996). The plot has been taken from Tozzi & Norman (2001). (*Right*): The low-z relation between X-ray luminosity and the mass contained within the radius encompassing an average density $200\rho_c$ (from Reiprich & Böhringer 2002). The two lines are the best log–log linear fit to two different data sets indicated with filled and open circles. The plot has been taken from Rosati et al. (2002).

Figure 1.8: β plotted against system temperature for 20 galaxy clusters and groups. The dashed line is $\beta = 2/3$ (Lloyd-Davies et al. 2000).

We saw in the earlier section § (1.2) that the dark matter profile in collapsed structures is universal and gas inside these structure follows dark matter. This fixes the value of β to be *unique* and a constant for all clusters ($\beta = 2/3$). The normalization of the density profile is fixed by scaling with the mass of the cluster.

However, observations showed large deviations from this — β was found to vary with cluster temperature or mass, as is seen in Figure (1.8). The value of β is smaller than predicted by self-similarity. This means that the density profiles are shallower as compared to theoretical predictions. This shows, again, that in reality, gas in galaxy clusters do not follow the simple scaling laws as dark matter does.

1.2.5.3 Entropy of the ICM

Another physical property of the intracluster gas which can be determined by X-ray measurements is the entropy. This is the entropy as defined for an ideal gas devoid of the logarithm and the constants. It is often referred to as the "adiabat". This is defined as

$$S = \frac{T_{\rm gas}}{n_e^{2/3}} \tag{1.11}$$

where $n_{\rm e}$ is the electron number density and $T_{\rm gas}$ is the temperature of the intracluster gas.

Following the self-similar scaling arguments (as stated earlier), $S \propto T_{\rm gas}$ since the mean density of gas, $\rho_{\rm gas} = const.$ at a particular epoch. Thus the entropy of a cluster should be proportional to the average weighted temperature of the system. However, observations show, yet again, that there are deviations from this simple scaling, as seen in Figure (1.9). It can be deduced from Figure (1.9) that rich clusters (above 4 keV) still follow this scaling but there are considerable deviations from this scaling for all clusters below 4 keV. It is also seen that there is a flattening in the relation between entropy and system temperature below $T_{\rm gas} < 2$ keV at around 100 keV cm^2. This was termed as the "entropy floor" in literature since there seemed to be a value of entropy below which it does not dip however much might the temperature of the cluster decrease.

Several authors have estimated the entropy of the ICM due to pure gravity at $0.1R_{\rm vir}$, ie. 10% of the virial radius by assuming that gas is in hydrostatic equilibrium with the background dark matter potential and follows the universal NFW profile which dark matter in clusters assume (Bryan 2000, Wu & Xue, 2002). They have also found that the entropy of the ICM due to gravity alone falls short of the observed entropy. The entropy excess observed is seen to increase with the decrease in cluster mass. However, as mentioned above, earlier data seemed to suggest an "entropy floor" below clusters of temperature 2 keV.

On the advent of new and better data for larger number of galaxy clusters and groups, this "entropy floor" vanished. It was established that this was more of an artifact due to the extrapolation which had to be done by Lloyd-Davies (2000) for the scarcity of low temperature systems (Ponman et al. 2003). This new data showed that the S–$T_{\rm gas}$ relation is shallower than the self-similar predictions ($S(0.1R_{\rm vir}) \propto T_{\rm gas}^{0.65}$ with no floor at 100 keV cm^2). This means that the gas is actually at a higher entropy level or higher adiabat than that predicted by these structure formation models. Thus the gas is probably heated by some mechanism other than gravity.

Figure 1.9: Gas entropy at $0.1R_{\rm vir}$ against system temperature for 20 galaxy clusters and groups. The dotted line is a $S \propto T_{\rm gas}$ fit to the systems above 4 keV (Lloyd-Davies et al. 2000).

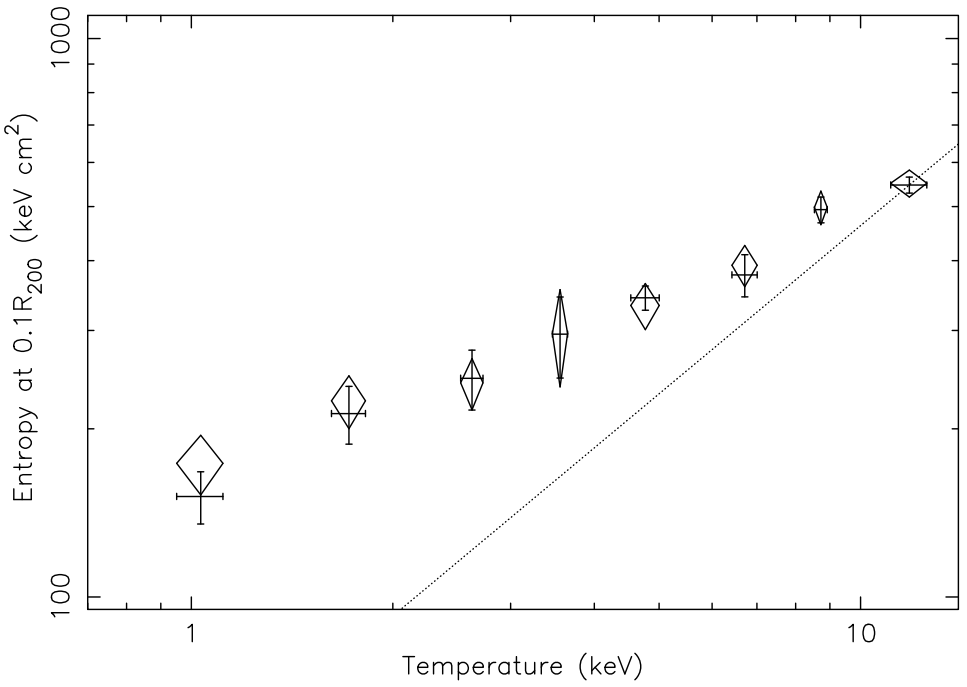

Figure 1.10: Binned data of 66 virialized clusters, rich and poor from Ponman et al. , 2003 showing gas entropy at $0.1R_{\rm vir}$ as a function of the cluster temperature . The solid line shows the self-similar scaling, $S \propto T_{\rm gas}$.

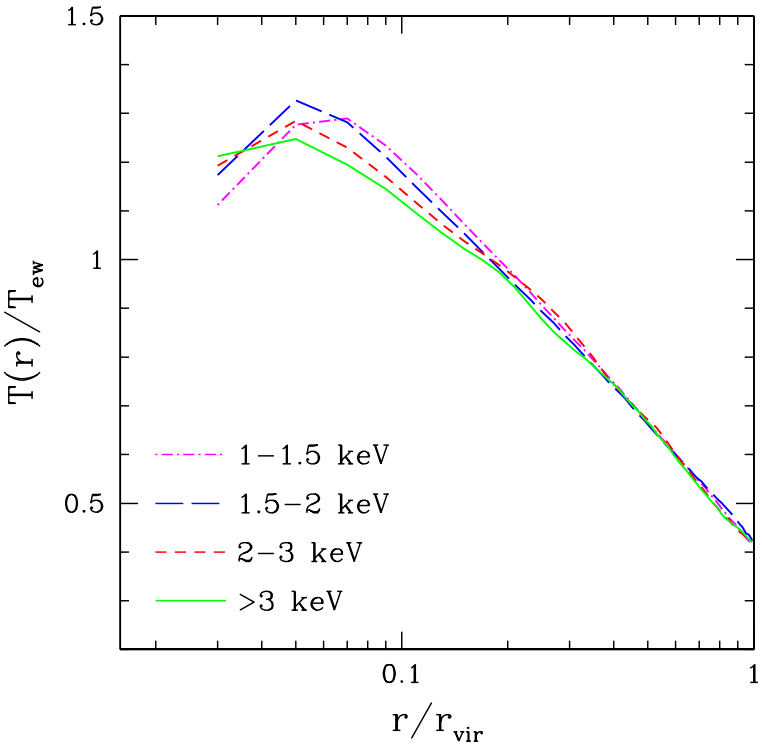

Figure 1.11: The average temperature profiles for groups and clusters within different interval of $T_{\rm ew}$, emission-weighted temperatures. This is a result of a hydrodynamical simulation by Borgani et al. 2004. They find the universal behaviour of the gas temperature profiles of clusters of different masses.

1.2.6 Departure from self-similarity in clusters

From the above comparisons of these observed scaling relations with the self-similar predictions, it is almost evident that self-similarity is broken in galaxy clusters. One of the reasons which is ascribed to the breaking of these scaling relations is heating of the intracluster gas at some earlier epoch by feedback from some non-gravitational astrophysical source like supernovae or AGNs. This was first suggested by Kaiser (1991) and he termed it as "pre-heating". It was also subsequently used by Evrard & Henry (1991) to explain the shape of the local X-ray luminosity function of clusters. This heating of the gas would increase the entropy of the ICM, place it on a higher adiabat, prevent it from reaching a high central density during the cluster gravitational collapse and, therefore, decrease the X-ray luminosity (see review by Rosati et al. 2002 and references therein).

Contrary to this pre-heating scenario, there is another scenario which was also suggested by several authors to explain this aberrant behaviour of clusters and groups from self-similarity. In this scenario, gas cooling is suggested to be the solution to this problem in poorer clusters and groups (Bryan 2000; Voit & Bryan 2001). This model is based on two simple ideas: (1) small clusters and groups have converted more of their baryonic gas into galaxies than have large clusters, and (2) the gas that goes to form the galaxies is preferentially lower in entropy, thus raising the mean entropy of the gas that remains. This means that not only do small clusters have a smaller gas fraction ($f_{\rm gas}$) but the gas that is there has a higher entropy – and lower density – than it would in simple self-similar scaling models. Because of the density-squared nature of the X-ray emission, this substantially diminishes the luminosity of groups and small clusters, resulting in a steeper $L_{\rm X}$–$T_{\rm gas}$ relation, as observed. The effective entropy increase is most noticeable in the centre of the cluster, which is just where the entropy floor is observed. This scenario, even though plausible, has become less favoured because of the larger observational evidence of AGN heating in clusters and also better estimates from X-ray of entropy profiles in clusters which indicate that there are deviations from self-similarity in all mass clusters, both rich and poor clusters.

The assumptions of adiabatic infall of gas in galaxy clusters leading to same scaling relations as the dark matter and also of isothermality are too simplistic. Recent numerical simulations of the intracluster medium with gravity alone show that the density structure of the intracluster gas does not follow the dark matter. The inclusion of the collisional terms in the physics of these baryons bring about changes in their final density profile from the background dark matter density profile. Also, observations show that clusters have temperature profiles and are not isothermal (Markevitch et al. 1998). More recently, the analysis of *Beppo*SAX observations accomplished by De Grandi & Molendi (2002) concluded that temperature profiles of galaxy clusters can be described by an isothermal core followed by a rapid decrease. Simulations of galaxy clusters also find that there is an "universal" behaviour of temperature profiles and are definitely not isothermal (Loken et al. 2002; Ascasibar et al. 2003, Borgani et al. 2004 and references therein).

Thus it can be concluded that the behaviour of the baryons inside galaxy clusters is complex. The gravitational interaction of these baryons with the background dark matter potential and the collisions among themselves lead them to have physical properties which are different from simple scaling laws obeyed by the collisionless dark matter. In addition, there are other processes in baryons like non-gravitational heating from other astrophysical sources inside galaxy clusters, radiative cooling,

thermal conduction and dissipation which lead them to have observable properties which scale in a very different fashion from self-similarity.

1.3 Pre-heating and the ICM

Pre-heating was first suggested by Kaiser (1991) to explain the strong negative evolution of clusters in X-ray surveys. In this scenario, the gas was assumed to experience some additional early heating from some astrophysical source before or as it fell into the cluster potential. The simple model which Kaiser (1991) suggested led to the prediction of a steeper $L_{\rm X}$–$T_{\rm gas}$ relation as compared to the self-similar one. A description of this model is as follows: at some early epoch, some agency (e.g. heating from supernova explosions) injected some additional energy into the gas and it was raised to an initial uniform temperature $T_{\rm i}$ and had density $\overline{\rho_{\rm i}} = (8\pi/3)\Omega_{\rm gas}H_{\rm i}^2$. These uniform density and temperatures are reasonable because conditions are atleast close to uniform when averaged over the mass scale of a present day rich cluster (a co-moving radius of $\simeq 10\ h^{-1}$ Mpc). Now this gas is at a higher temperature than the virial temperature of the dark matter clumps existing then and would thus be unperturbed mostly by the dark matter clustering. However, as time goes on, the gas temperature will cool adiabatically with $T \propto a^{-2}$ (a being the scale factor), the potential wells will deepen and the gas will become inhomogeneous and settle into these evolving potential wells approximately adiabatically. Shocks, if any, would be very weak. With these assumptions, Kaiser (1991) showed that $L_{\rm X} \propto \Phi^{7/2} \propto T_{\rm gas}^{7/2}$ where Φ is the gravitational potential of the dark clump $\propto T_{\rm gas}$ (see Appendix B for full derivation).

Subsequently, this pre-heating scenario was adopted by several other authors to explain the entropy and X-ray luminosity observations in more recent times. Early pre-heating by non-gravitational sources like supernovae driven galactic winds, quasars and radio galaxies would lead to the increase in the entropy of the gas, place it on a higher adiabat, prevent it from reaching a high central density during the cluster gravitational collapse and, therefore, settle into a shallower density profile. This would decrease the X-ray luminosity and make the entropy of this gas higher than the expectations due to just pure gravitational infall without preheating (e.g. Metzler & Evrard 1994; Navarro J. F., Frenk et al. 1995; Bower R. G. 1997; Cavaliere et al. 1997; Ponman et al. 1999; Balogh et al. 1999; Tozzi & Norman 2001 and references therein). For a fixed amount of extra energy per gas particle, this effect is more prominent for poorer clusters, i.e., for those objects whose virial temperature is comparable with the extra-heating temperature. As a result, the self-similar behaviour of the ICM is expected to be preserved in rich clusters, whereas it is broken for colder systems. Both semi-analytical works (e.g. Cavaliere et al. 1998; Balogh et al. 1999; Wu et al. 2000; Tozzi et al. 2001) and numerical simulations (e.g. Navarro et al. 1995; Brighenti & Mathews 2001; Bialek et al. 2001; Borgani et al. 2001) have indicated that $\simeq 1$ keV/particle of extra energy is required to reconcile with $L_{\rm X}$–$T_{\rm gas}$ and S–$T_{\rm gas}$ observations. The idea of early heating by some non-gravitational source like star formation, Pop III stars, supernovae and AGNs is attractive because the gas density is low then and so the entropy can be increased with a smaller energy expenditure per particle. However, several authors now have also addressed this problem by suggesting that the gas is being currently heated by active AGNs and quasars residing inside clusters (see chapter (3)).

1.3.1 Supernovae and ICM heating

One of the most energetic explosive events ever known is a supernova. These occur at the end of a star's lifetime, when its nuclear fuel is exhausted and it is no longer supported by the release of nuclear energy. If the star is particularly massive, then its core will collapse and in so doing will release a huge amount of energy. This will cause a blast wave that ejects the star's envelope into interstellar space. The result of the collapse may be, in some cases, a rapidly rotating neutron star that can be observed many years later as a radio pulsar.

There are two types of supernovae identified from their light curves: Type I and Type II. Type I exhibit a sharp maximum in luminosity and then have a gradual decline with time. Type II exhibit a broader peak at maximum and then decline more quickly. The spectra of type II supernova do not show lines of H which means that they come from highly evolved objects. The basic models for Type I and Type II are:

Type I - a binary model (red giant and white dwarf) where the accreted mass is so high it pushes the white dwarf over the chandrashekar limit. The core collapses igniting the carbon in one big burst. The star blows itself to bits and no remnant remains.

Type II - a massive star burns all its fuel up until iron and collapses.

In clusters, it is Type II supernovae which is thought to be the candidates which can drive galactic winds and heat the intracluster medium. Thus in the context of the intracluster medium, it is believed that star formation would proceed rapidly in cold gas inside galaxies which would lead to Type II supernovae. This is assumed to continue until the energy from supernovae is sufficient to eject the remaining gas out of the halo, or until the cold gas is used up. Gas that is ejected from a galaxy, as seen in Figure (1.12), is expected to re-collapse within the same potential well and be a part of the intracluster medium (Wu et al. 1998, 2000). The energy per supernova available for the ejection of gas is approximately $\simeq 4 \times 10^{50}$ erg (Spitzer 1978). Although the total energy released by a supernova is typically $\simeq 10^{51}$ erg, a large fraction of this is likely to be radiated, especially if the supernova explodes in cold gas (Wu et al. 2000). The presently most reliable diagnostic of supernova heating in clusters – that presumably occurred during star formation-driven galactic outflows at early epochs – is the ICM silicon abundance. Only iron abundances are determined more accurately; however, the amount of energy ejection associated with the mass of Fe in the ICM is sensitive to the poorly determined (e.g., Gibson et al. 1997) relative fractions of Fe originating from Type Ia (SNe Ia) and Type II (SNe II) supernovae. Not only have accurate Si abundances been determined for a large sample of clusters (Fukazawa et al. 1998), but the explosion energy per Si yield is similar in standard SN Ia and SN II models (e.g., Gibson et al. 1997). The equivalent temperature of the injected energy can be expressed as

$$k_{\rm b} T_{\rm eq}^{\rm SN} = 1.6\, Z_{\rm Si}\, e_{\rm SN}\ {\rm keV}\,, \tag{1.12}$$

where $Z_{\rm Si}$ is the ICM Si abundance, relative to solar, and $e_{\rm SN}$ is the average injected energy per supernova in units of 10^{51} erg (Loewenstein 2000).

Thus the global-average heating is of the order of 1 keV per particle if $e_{\rm SN} \sim 1$ since the Si

Figure 1.12: This image highlights the the galactic wind coming out from this remarkable star-burst galaxy, M82. This is a result of violent star formation and blasts from supernova explosions which have created a billowing cloud of expanding gas emerging from the galaxy. This image is a result of combining a wide field image from the WIYN Telescope in Arizona with a smaller high-resolution image from the orbiting Hubble Space Telescope. **Credit: M. Westmoquette (UCL), J. Gallagher (U. Wisconsin-Madison), L. Smith (UCL), WIYN/NSF, HST, NASA/ESA.**

abundance in rich clusters is $\simeq 0.7$ (Fukazawa et al. 1998) and is around $\simeq 0.3$ in poor clusters and groups (Davis et al. 1999; Hwang et al. 1999). This however requires a very high energy-deposition efficiency into the ICM. Roughly, the efficiency for the energy released in a supernova explosion to convert into mechanical energy which would drive the galactic wind is thought to be around 1/10th - 1/100th which makes the average energy deposited per particle become $\simeq 0.1$ keV-0.01 keV. Thus it can be seen that the excess energy required in clusters and groups of galaxies far exceeds the energy which can be deposited by supernovae driven outflows (Valageas & Silk 1999; Kravtsov & Yepes 2000).

1.3.2 Active galactic nuclei and the intracluster medium

Active galactic nuclei (abbreviated as 'AGN') are galaxies which have a small core of emission embedded in an otherwise typical galaxy. This core may be highly variable and very bright compared to the rest of the galaxy. Models of active galaxies concentrate on the possibility of a super-massive black hole (10^6 to 10^9 $M_\odot$) which lies at the center of the galaxy. The dense central parts of the galaxy provide material which accretes onto the super-massive black hole releasing large amount of gravitational and electromagnetic energy.

There are several types of active galaxies: Seyferts, quasars, blazars and radio-galaxies. In ~10% of the AGN, the super-massive black hole and the accretion disk produce narrow beams of energetic particles and magnetic fields, and eject them outward in opposite directions away from the disk. These are the jets, which emerge at nearly the speed of light. Radio galaxies, quasars, and blazars are AGNs with strong jets, which can travel outward into large regions of intergalactic space. Many of the

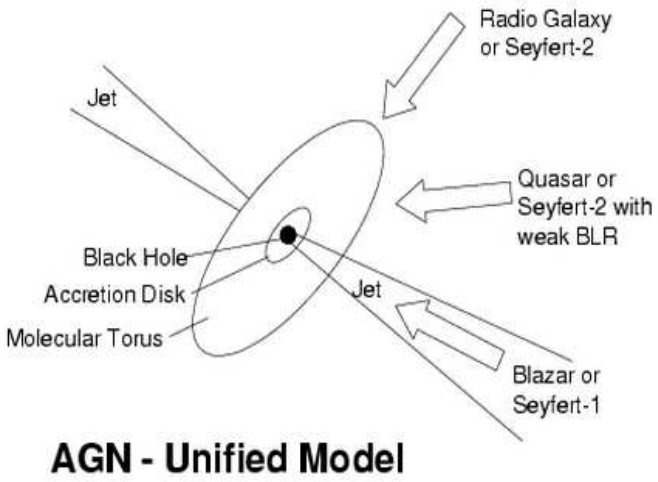

apparent differences between types of AGN are due to our having different orientations with respect to the disk. With Blazars and Quasars, the line of sight is down and along the jet axis. For Seyferts, the jet is being viewed broadside. AGNs release large amounts of energy to their environments, in several forms. In luminous AGNs such as Seyfert nuclei and quasars, the most obvious output is radiative and this affects the environment through both radiation pressure and radiative heating. Although jets and winds are usually associated with radio galaxies, which often release the bulk of their power in this form (Rees et al. 1982; Begelman, Blandford, & Rees 1984), recent theoretical and observational developments suggest that most accreting black holes can also produce substantial outflows. Numerical simulations suggest that accretion disks, which transfer angular momentum and dissipate binding energy via magneto-rotational instability, may inevitably produce magnetically active coronae (Miller & Stone 2000). These are likely to generate outflows that are further boosted by centrifugal force (Blandford & Payne 1982). Outflows in broad absorption-line (BAL) QSOs (Arav & Li 1994; Arav, Li, & Begelman 1994; Murray et al. 1995) have shown circumstantial evidence for acceleration by radiation pressure (Arav 1996; Arav et al. 1999). In addition, they could also be boosted hydro-magnetically. Whatever the acceleration mechanism(s), these winds are probably accelerated close to the central engine, and therefore should be regarded as part of the kinetic energy output. New spectral analyses of BAL QSOs, made possible by observations with the *Hubble Space Telescope*, imply that the absorption can be highly saturated (Arav et al. 2001) and may originate far from the nucleus (de Kool et al. 2001). This indicates that the kinetic energy in the BAL outflows is larger than previously thought and can approach the radiation output. Moreover, new evidence suggests that relativistic jets are common or ubiquitous in X-ray binaries containing black hole candidates. While the energetics of these outflows are not yet fully established, their environmental impacts may be substantial (Heinz 2002).

At an energy conversion efficiency of ϵc^2 per unit of accreted mass, an accreting black hole liberates $10^{19}(\epsilon/0.01)$ erg per gram (Begelman 2001). In principle the efficiency could be ~ 6 to more than 40 times larger than this (depending on the black hole spin and boundary conditions near the event horizon: Krolik 1999; Agol & Krolik 2000), but the estimate quoted above is the most conservative one. Here, ϵ can be seen as the efficiency of kinetic energy production, since this is probably the most

effective means by which black holes affect their surroundings. Under many circumstances, feedback via kinetic energy injection can be quite efficient. Both radiative heating and acceleration by radiation pressure, on the other hand, have built-in inefficiencies. In both photo-ionization heating and Compton heating, only a fraction of the photon energy goes into heat, the majority being re-radiated.

However, the efficacy of kinetic energy injection depends on the structure of the medium in which it is deposited. The speed of a shock or sound wave propagating through a medium will be highest with the lowest density structure. Dense regions will be overrun and left behind by the front, as first pointed out by McKee & Ostriker (1977) in connection with supernova blast waves propagating into the interstellar medium. Consequently, most of the energy goes into the gas which has the lowest density (and is the hottest) to begin with. The global geometric structure of the ambient gas is important as well. Since a wind or hot bubble emanating from an AGN will tend to follow the "path of least resistance," a disk-like structure can lead to a "blowout" of the hot gas along the axis. A more spherically symmetric gas distribution will tend to keep the AGN energy confined in a bubble (Begelman 2001 and references therein).

AGN feedback due to kinetic energy injection is perhaps most evident in clusters of galaxies. Recent observations of intracluster gas by *Chandra* and *XMM-Newton* indicate that some energy source is quenching so-called "cooling flows" in clusters of galaxies (Allen et al. 2001; Fabian et al. 2001; Peterson et al. 2001). Energy injected by intermittent radio galaxy activity at the cluster center is the most likely source. This is specially important because 70% of cooling flow clusters harbour radio galaxies in their centres (Burns 1990). This same form of energy input, spread over larger scales, could also be the source of *non-gravitational heating* in galaxy clusters and groups (Valageas & Silk 1999; Nath & Roychowdhury 2002). In the life-time of a radio-galaxy, with the jet being active for around $\sim 10^7$ years, the energy released is typically $\sim 10^{60}$ erg. This is typically $\simeq$ the amount of total energy required by a cluster if the excess energy required to satisfy observations is ~ 1 keV/particle (assuming that the electron density of the ICM is $n_e \simeq 10^{-2}$ cm^{-3} and volume of the cluster is $V_{cl} \simeq (4/3)\pi\,(1\ \mathrm{Mpc})^3$).

There are different phases in the evolution of a radio galaxy. They evolve through three stages where only the first of which are dominated by the jet momentum. Although the radio morphologies in powerful (Fanaroff-Riley class II) sources are dominated by the elongated lobes and compact hotspots, most of the energy accumulates in a faint "cocoon" that has a thick cigar-like shape (Blandford & Rees 1974; Scheuer 1974). The same is probably true of the weaker FR I sources, which appear to be dominated by emission from turbulent regions along the jet. The over-pressured cocoons (with respect to the ambient medium) drives a shock "sideways" at the same time as the jets are lengthening their channels by depositing momentum. The sideways expansion catches up with the lengthening very soon. Dynamically, active radio galaxies with over-pressured cocoons resemble spherical, supersonic stellar wind bubbles (Castor, McCray & Weaver 1975; Begelman & Cioffi 1989). Soon after the evolution is dominated by buoyancy when the pressures inside the cocoon has equilibrated with the ambient medium (Gull & Northover 1973). Cygnus A, which has been expanding for several million years now, is hundreds of kpc across and is still over-pressured by a factor $\sim$ 2–3 with respect to the ambient medium (Smith et al. 2002). However most radio galaxies found in clusters seem to have evolved into the buoyancy-driven stage fairly early. The direct influence of a radio galaxy on its surroundings does not end with the end of the momentum-driven stage and the onset of the buoyancy-

driven stage. Buoyant bubbles of hot, relativistic plasma can "rise" for considerable distances inside the cluster atmosphere maintaining their identity and spreading the AGN's energy output widely.

Recent X-ray observations by *Chandra* and *XMM-Newton* has detected such buoyant bubbles as X-ray depressions or 'X-ray holes' bounded by bright (cool) rims. Some examples of clusters where such depressions have been observed are Perseus (Fabian et al. 2003), Hydra A (McNamara et al. 2000), MKW 3s (Mazzotta et al. 2002) and many others. Recently, Bîrzan et al. 2004 reported the presence of X-ray holes or depressions associated with a central radio galaxy in $\sim$ 16 clusters. Simulations and analytical calculations also show that such bubbles can exist and buoyantly rise up in the cluster atmosphere (Churazov et al. 2001; Brüggen & Kaiser 2001 and many others). These bubbles can do more than just offset radiative losses in the cores of clusters. They can rise up to larger radii in clusters and inject energy into the intracluster medium. Thus "bubble heating" can be formulated as one of the sources for non-gravitational heating in clusters.

1.4 Motivation

In the earlier sections § (1.1) and § (1.2), we saw that clusters of galaxies and the intracluster medium have been studied in detail by several authors through last several decades. Yet, with the advent of better X-ray telescopes, new facts are being discovered about the intracluster medium which have raised new issues or have raised questions about our understanding of certain old issues. One such issue is the departure of the baryonic gas inside clusters from self-similar scaling laws predicted from structure formation theories. Numerical simulations are slowly acquiring a stage where they can address issues related to non-linear collapse of objects and the gravitational interaction of gas and dark matter. However X-ray observations still show departures from the theoretical predictions which assume that gravitational interactions alone determine all physical properties and dynamics of baryons in clusters. This has led to the suggestion that the gas inside clusters is influenced by non-gravitational processes. In the last section § (1.3), we saw that one such process is pre-heating of the baryonic gas before or as it fell into the gravitational potential of dark clumps by astrophysical sources like supernovae driven outflows, AGNs and violent star-formation.

The main motivation of this thesis is to address this issue of non-gravitational heating from active galactic nuclei and quantify the energetics of this process. In doing this, we have first modeled the intracluster medium in hydrostatic equilibrium with the background dark matter potential to quantify the state of the gas due to pure gravity. This was done to re-estimate the exact requirement of excess energy from non-gravitational sources to reconcile with recent detailed and improved X-ray observations. Using this new estimate of the excess energy/entropy required to reconcile with observations, we have devised models by which AGNs and their bubbles can heat the intracluster medium and have shown that the recent observations can be satisfied by AGN heating. In our first model of AGN heating, we have evaluated the statistics of AGNs in clusters and groups. We have used a simple model of heating of the ICM by mechanical work done by jets as they expand into the ICM and by over-pressured cocoons to quantify the total excess energy which AGNs can deposit into the intracluster gas as a function of the cluster mass and temperature. This model considers only the first two violent phases of AGN activity where the jet is active and the cocoon expands into the ICM as it is over-pressured compared to the ambient medium. However, in our next models of AGN heating,

we consider the more quiescent phase of AGN activity where the heating is gentle. This heating is due to the expansion of buoyant bubbles as they rise in the ICM due to the pressure gradient. Infact, this phase is also seen to be quite an important phase in the life-time of an AGN and can add to the total mechanical energy an AGN can contribute to the ICM. We have modeled this phase of AGNs to explore the possibility of heating the ICM by such bubbles arising out of few active phases of a single central AGN inside the cluster. Such models have become very plausible and attractive since they are thought to be important in solving the problem of precipitous radiative cooling in the centres of clusters. Infact, it is believed that these AGNs, which are mostly found to in the central galaxy in clusters, are fueled by accretion from cooling flows. This triggers the AGN to become active again. Thus they go through several such active and quiescent cycles and regulate cooling flows in clusters (Kaiser & Binney (2003)).

1.5 Layout of the thesis

Chapter 2: In this chapter, we address the issue of quantification of excess entropy or energy, over and above the gravitational entropy or energy of the ICM, required to satisfy observations. We estimate the density profile of intracluster gas using the "universal temperature profile" and hydrostatic equilibrium. We compare the earlier estimates of gas entropy profiles, X-ray luminosity, gas fraction and so on, using self-similar density profiles, with our new estimates.

Chapter 3: In this chapter, we model quasar outflows and estimate the energy which a single quasar can contribute to the surrounding medium. In addition, we also estimate the number of quasars or AGNs that can reside inside a cluster of some mass ie. we derive the mass function of quasars inside clusters. Using these facts, we finally estimate the total excess energy which can be contributed by a population of quasars inside a cluster. We show that the amount of excess energy required in clusters and groups from non-gravitational sources to reconcile with observations can be wholly provided by radio-galaxies and BAL quasars.

Chapter 4: In Chapter (4), we model the heating due to buoyant bubbles from an active galactic nuclei of the ICM. We consider two models of AGN heating here: one where "effervescent heating" is combined with convection and radiative cooling and the other where "effervescent heating" is combined with thermal conduction and cooling. We show that AGNs in this phase of their life, which is very gentle and have hardly any strong outflows, can also provide mechanical energy into the surrounding medium. We show that this energy is enough to heat the medium and raise its entropy so much so that it can satisfy the observed entropy values.

Chapter 5: Finally in this chapter, we explore the ramifications of such heating via "effervescent mechanism" and thermal conduction of the intracluster gas on another observable property of the ICM, the thermal Sunyaev-Zel'dovich effect. We find that our heating models have some predictions which can be verified with new upcoming telescopes which are going to look at SZ effect from clusters. Infact, we see that non-gravitational heating in clusters would have considerable effects on the SZ temperature decrements and thus these observations can serve as another important constraint on such heating models of clusters.

Bibliography

Abell G. O., 1958, ApJS, 3, 211

Agol E., & Krolik, J. H., 1999, ApJ, 528, 161

Allen S. W. et al. , 2001, MNRAS, 324, 842

Allen S. W., & Fabian A. C., 1998, MNRAS, 297, 57

Arav N., & Li Z. Y., 1994, ApJ, 427, 700

Arav N., Li Z. Y., & Begelman M. C. 1994, ApJ, 432, 62

Arav N., 1996, ApJ, 465, 617

Arav N. et al. ., 2001, ApJ, 561, 118

Arav N., Korista K. T., de Kool M., Junkkarinen V. T., & Begelman, M. C., 1999, ApJ, 516, 27

Arnaud M., & Evrard A. E., 1999, MNRAS, 305, 631

Ascasibar Y., Yepes G., Müller V., & Gottlöber S., 2003, MNRAS, 346, 731

Ascasibar Y., Yepes G., Gottlöber S., & Müller V., 2004, MNRAS, 352, 1109

Balogh M. L., Babul A., Patton D. R., 1999, MNRAS, 307, 463

Bardeen J. M., Bond J. R., Kaiser N., & Szalay A. S., 1986, ApJ, 304, 15

Begelman M. C., 2001, in Gas and Galaxy Evolution, ed. J. E. Hibbard, M. P. Rupen, & J. H. van Gorkum (San Francisco: ASP), 363

Begelman M. C., & Cioffi D. F., 1989, ApJ, 345, 21

Begelman M. C., Blandford R. D., & Rees M. J., 1984, Rev. Mod. Phys., 56, 255

Bialek J. J., Evrard A. E., & Mohr J. J., 2001, ApJ, 555, 597

Bîrzan L., Rafferty D. A., McNamara B. R., Wise M. W., & Nulsen P. J. E., 2004, ApJ, 607, 800

Blandford R. D., & Rees M. J., 1974, MNRAS, 169, 395

Blandford R. D., & Payne D. G., 1982, MNRAS, 199, 883

Blumenthal G. R., Faber S. M., Primack J. R., & Rees M. J., 1984, Nature, 311, 517

Borgani S. et al. , 2001, ApJ, 551, 71

Borgani S. et al. , 2004, MNRAS, 348, 1078

Bower R. G., 1997, MNRAS, 288, 355

Bradt H., Mayer W., Naranan S., Rappaport S., & Spada G., 1967, ApJ, 150, 199

Bridle A. H., & Feldman P., 1972, Nature, 235, 168

Brecher K., & Burbidge G. R., 1972, Nature, 237, 440

Brüggen M., & Kaiser, C. R., 2002, Nature, 418, 301

Bryan G. L., 2000, ApJ, 540, 39

Bryan G. L., 2000, ApJ, 544, L1

Bryan G. L., & Norman M. L., 1998, ApJ, 495, 80

Burns J. O., 1990, AJ, 99, 14

Byram E. T., Chubb T. A., Friedman H., 1966, Science, 152, 66

Canizares C. R., 1999, Ap&SS, 267, 251

Cavaliere A., Gursky H., & Tucker W., 1971, ApJ, 231, 437

Cavaliere A., Fusco-Femiano R., 1976, A&A, 49, 137

Cavaliere A., Menci N., Tozzi P., 1997, ApJ, 484, 21

Castor J. I., Abbott D. C., & Klein, R. I., 1975, ApJ, 195, 157

Churazov E., Brüggen M., Kaiser C. R., Böhringer, H., & Forman, W., 2001, ApJ, 554, 261

Coles P., Lucchin F., 2002, Cosmology: the origin and evolution of cosmic structure, 2nd ed. Chichester, England, John Wiley & Sons

Costain C. H., Bridle A. H., Feldman P. A., 1972, ApJ, 175, 15

Crone M. M., Evrard A. E., & Richstone D. O., 1994, ApJ, 434, 402

David L. P., Slyz A., Jones C., Forman W., Vrtilek S. D., & Arnaud K. A., 1993, ApJ, 412, 479

Davis M., Efstathiou G., Frenk C. S., & White S. D. M., 1985, ApJ, 292, 371

Davis D. S., Mulchaey J. S., & Mushotzky R. F., 1999, ApJ, 511, 34

De Grandi S., Molendi S., 2002, ApJ, 567, 153

de Kool M., Arav N., Becker R. H., Gregg M. D., White R. L., Laurent-Muehleisen S. A., Price T., & Korista K. T., 2001, ApJ, 548, 609

Dressler A., 1984, ARA&A, 22, 185

Dubinski J. & Carlberg R. G., 1991, ApJ, 378, 496

Edge A. C., & Stewart G. C., 1991, MNRAS, 252, 428

Elvis M., 1976, MNRAS, 177, 7

Evrard A. E., & Henry J. P., 1991, ApJ, 383, 95

Evrard A. E., Metzler C. A., & Navarro, J. F., 1996, ApJ, 469, 494

Fabian A. C., 1994, ARA&A, 32, 277

Fabian A. C., Pringle J. E., Rees M. J., 1976, Nature, 263, 301

Fabian A. C., Mushotzky R. F., Nulsen P. E. J., & Peterson, J. R., 2001, MNRAS, 321, 20

Fabian A. C., Sanders J. S., Allen S. W., Crawford C. S., Iwasawa K., Johnstone R. M., Schmidt R. W. & Taylor G. B., 2003, MNRAS, 344, 43

Fabricant D., Kent S., & Kurtz M., 1989, ApJ, 336, 77

Fahlman G., Kaiser N., Squires G., & Woods D., 1994, ApJ, 437, 56

Felten J. E., Gould R. J., Stein W. A., Woolf N. J., 1966, ApJ, 146, 955

Fillmore J. A., & Goldreich P., 1984, ApJ, 281, 1

Flores R. A., & Primack J. R., 1994, ApJ, 427, 1

Frenk C. S., White S. D. M., Davis M., Efstathiou G., 1988, ApJ, 327, 507

Forman W., Kellogg E., Gursky H., Tananbaum H., & Giacconi R., 1972, ApJ, 178, 309

Forman W., & Jones C., 1982, ARA&A, 20, 547

Fort B., Prieur J. L., Mathez G., Mellier Y., Soucail G., 1988, A&A, 200, 17

Fort B., & Mellier Y., 1994, A&ARv., 5,239

Fritz G., Davidsen A., Meekins J. F., & Friedman H., 1971, ApJ, 164, 81

Fukazawa Y., Makishima K., Tamura T., Ezawa H., Xu H., Ikebe Y., Kikuchi K., & Ohashi T., 1998, PASJ, 50, 187

Fukushige T., & Makino J., 1997, ApJ, 477, 9

Fukushige T., & Makino J., 2001, ApJ, 557, 533

Fukushige T., & Makino J., 2003, ApJ, 588, 674

Ghinga S., Moore B., Governato F., Lake G., Quinn T., Stadel J., 1998, MNRAS, 300, 146

Ghinga S., Moore B., Governato F., Lake G., Quinn T., Stadel J., 1998, ApJ, 544, 616

Giacconi R., Murray S., Gursky H., Kellogg E., Schreier E., & Tananbaum, H., 1993, ApJ, 178, 281

Gibson B. K., Loewenstein M., & Mushotzky R. F., 1997, MNRAS, 290, 623

Gioia I. M., Shaya E. J., Le Fèvre O., Falco, E. E., Luppino G., Hammer F., 1998, ApJ, 497, 573

Gunn J. E., 1977, ApJ, 218, 592

Gunn J. E., & Gott J. R. I., 1972, ApJ, 176, 1

Gull S. F., & Northover K. J. E., 1973, Nature, 224, 80

Gursky H., Kellogg E., Leong C., Tananbaum H, & Giacconi R., 1971a, ApJ, 165, 43

Gursky H., Kellogg E., Murray S., Leong C., Tananbaum H., & Giacconi R., 1971b, ApJ, 167, 81

Hammer F., & Rigaud F., 1989, A&A, 226, 45

Hammer F., Teyssandier P., Shaya E. J., Gioia I. M., Luppino G. A., 1997, ApJ, 491, 477

Harris D. E., & Romanishin W., 1974, ApJ, 188, 209

Heinz S., 2002, A&A, 388, 40

elsdon S. F., & Ponman T. J., 2003, MNRAS, 340, 485

Henriksen M., & Mamon G., 1994, ApJ, 421, 63

Henry P., Briel U., & Nulsen P., 1993, A&A, 271, 63

Hwang U., Mushotzky R. F., Burns J. O., Fukazawa Y., & White R. A., 1999, ApJ, 516, 604

Jones C., & Forman W., 1984, ApJ, 276, 38

Jing Y. P., & Suto Y., 2000, ApJ, 529, 69

Kaiser N., 1984, ApJ, 284, 9

Kaiser N., 1986, MNRAS, 222, 323

Kaiser N., 1991, ApJ, 383, 104

Kaiser N., & Squires G., 1993, ApJ, 404, 441

Kaiser C. R., Binney J., 2003, MNRAS, 338, 837

Karzas W. J., & Latter R., 1961, ApJS, 6, 167

Katz J. I., 1976, ApJ, 207, 25

ayser R., Schramm T., & Naiser L., 1992, Gravitational Lenses, Springer-Verlag

Kellogg E., Baldwin J. R., Koch D., 1975, ApJ, 199, 299

King I., 1962, AJ, 67, 471

Klypin A., Kravtsov A. V., Bullock J. S., Primack J. R., 2001, ApJ, 554, 903

Kneib J. P., Mellier Y., Fort B., Mathez, G., 1993, A&As, 273, 367

Kneib J. P., Mellier Y., Pelló R., Miralda-Escudé J., Le Borgne J. F., Böhringer H., Picat J. P., 1995, A&A, 303, 27

Kneib J.-P., Ellis R. S., Smail I., Couch W., Sharples R. M., 1996, ApJ, 471, 643

Kravtsov A. V., Yepes G., 2000, MNRAS, 318, 227

Krolik J. H., 1999, ApJ, 515, 73

Lloyd-Davies E. J., Ponman T. J., Cannon D. B., 2000, MNRAS, 315, 689

Łokas E. L., & Hoffman Y., 2000, ApJ, 542, 139

Loken C., Norman M. L., Nelson E., Burns J., Bryan G. L., Motl P., 2002, ApJ, 579, 571

Lynden-Bell D., 1967, MNRAS, 136, 101

Marchesini D., DÓnghia E., Chincaini G., Firmani C., Conconi P., Molinari E., & Zacchei A., 2002, ApJ, 575, 801

Markevitch M., Forman W. R., Sarazin C. L., Vikhlinin A., 1998, ApJ, 503, 77

Matthews T. A., Morgan W. W., & Schmidt M. 1964, ApJ, 140, 35

Mazzotta P., Kaastra J. S., Paerels F. B., Ferrigno C., Colafrancesco S., Mewe R., & Forman W. R., 2002, ApJ, 567, 37

McKee C. F., & Ostriker J. P., 1977, ApJ, 218, 148

McNamara B. R., Wise M., Nulsen P. E. J., David L. P., Sarazin C. L., Bautz M., Markevitch M., Vikhlinin A., Forman W. R., Jones C., & Harris D. E., 2000, ApJ, 534, 135

Meekins J. F., Gilbert F., Chubb T. A., Friedman H., & Henry R. C., 1971, Nature, 231, 107

Mellier Y., 1999, ARA&A, 37, 127

Mellier Y., Fort B., & Kneib J. P., 1993, ApJ, 407, 33

Metzler C. A. & Evrard A. E., 1994, ApJ, 437, 564

Miller K. A., & Stone J. M., 2000, ApJ, 534, 398

Minkowski R., & Abell G. O., 1963, PASP, 75, 488

Miralda-Escude J., 1995, ApJ, 438, 514

Mitchell R. J., Culhane, J. L., Davison P. J. N., & Ives J. C., 1976, MNRAS, 175, 29

Mitchell R. J., Dickens R. J., Burnell S. J. B., Culhane J. L., 1979, MNRAS, 189, 329

Moore B., Governato F., Quinn T., Stadel J., & Lake G., 1998, ApJ, 499, 5

Moore B., Quinn T., Governato F., Stadel J, & Lake G., 1999, MNRAS, 310, 1147

Mulchaey J. S., 2000, ARA&A, 38, 289

Mulchaey J. S., Davis, D. S., Mushotzky R. F., Burstein D., ApJ, 404, 9

Murray N., Chiang J., Grossman S. A., & Voit G. M., 1995, ApJ, 451, 498

Navarro J. F., Frenk C. S., White S. D. M., 1995, MNRAS, 275, 720

Navarro J. F., Frenk, C. S., & White S. D. M., 1996, ApJ, 462, 563

Navarro J. F., Frenk C. S., & White S. D. M., 1997, ApJ, 490, 493

Nath B. B., & Roychowdhury S., 2002, MNRAS, 333, 145

Padmanabhan T., 1993, Structure formation in the universe, Cambridge, UK, Cambridge University Press

Oegerle W. R., & Hill J. M., 1994, AJ, 107, 857

Perola G. C., Reinhardt M., 1972, A&A, 17, 432

Ponman T. J., & Bertram D., 1993, Nature, 363, 51

Ponman T. J., Allan D. J., Jones L. R., Merrifield M., McHardy I. M., Lehto H. J., Luppino G. A., 1994, Nature, 369, 462

Ponman T. J., Bourner P. D. J., Ebeling H., & Böhringer H., 1996, MNRAS, 283, 690

Ponman T. J., Cannon D. B., Navarro J. F., 1999, Nature, 397, 135

Ponman T. J., Sanderson A. J. R., Finoguenov A., 2003, MNRAS, 343, 331

Peacock J. A., 1999, Cosmological Physics, Cambridge University Press, Cambridge, UK

Peebles P. J. E., 1982, ApJ, 263, 1

Peebles P. J. E., 1993, Principles of physical cosmology, Princeton Series in Physics, Princeton, NJ, Princeton University Press

Pello R., Sanahuja B., Le Borgne J. F., Soucail G., & Mellier Y., 1991, ApJ, 366, 405

Peterson J. R. et al. , 2001, A&A, 365, 104

Quinn P. J., Salmon J. K., Zurek W. H., 1986, Nature, 322, 329

Rees M. J., Begelman M. C., Blandford R. D., & Phinney E. S., 1982, Nature, 295, 17

Reiprich T. H., Böhringer H., 2002, ApJ, 567, 716

Rephaeli Y., 1977a, ApJ, 212, 608

Rephaeli Y., 1977b, ApJ, 218, 323

Rees M. J., & Ostriker J. P., 1977, MNRAS, 179, 541

Rosati P., Borgani S., Norman C., 2002, ARA&A, 40, 539

Sarazin C. L., 1988, X-Ray Emissions from Clusters of Galaxies, Cambridge. Cambridge Univ. Press

Scheuer P. A. G., 1974, MNRAS, 166, 513

Schneider P., Ehlers J., & Falco E., 1992, Gravitational Lenses, Springer-Verlag

Serlemitsos P. J., Smith B. W., Boldt E. A., Holt S. S., & Swank J. H., 1977, ApJ, 211, 63

Shapiro P. R., Iliev I. T., 2000, ApJ, 542, 1

Smail I., 1993, Gravitational Lensing by Rich Clusters of Galaxies, PhD Thesis

Smith S., 1936, ApJ, 83, 23

Smith D. A., Wilson A. S., Arnaud K. A., Terashima Y., & Young A. J., 2002, ApJ, 565, 195

Spitzer L, 1978, Physical Processes in the Interstellar Medium, Wiley Interscience, New York

Tornatore L., Tozzi P., 2004, MNRAS, 348, 107

Tozzi P., Norman C., 2001, ApJ, 546, 63

Tyson J. A., Valdes F., & Wenk R. A., 1990, ApJ, 349, 1

Tyson J. A., Kochanski G. P., Dell' Antonio I. P., 1998, ApJ, 498, 107

Valageas P., & Silk J., 1999, A&A, 350, 725

Voit G. M., Bryan G. L., 2001, Nature, 414, 425

White S. D. M., & Rees M. J., 1978, MNRAS, 183, 341

Wolf M., 1906, Astron. Nachr., 170, 211

Wu K. K. S., Fabian A. C., & Nulsen P. E. J., 1998, MNRAS, 301, 20

Wu X. P., Xue Y. J., Fang L. Z., 1999, ApJ, 524, 22

Wu X., Xue Y., 2002, ApJ, 569, 112

Wu K. K. S., Fabian A. C., & Nulsen P. E. J., 2000, MNRAS, 318, 889

Zaroubi S., Naim A., & Hoffman Y., 1996, ApJ, 457, 50

Zwicky F., 1937, ApJ, 86, 217

Zwicky F., Herzog E., Wild P., Karpowicz M., & Kowal C. T., 1961 - 1968, Catalogues of Galaxies and Clusters of Galaxies, Vol. 1-6, Pasadena: Caltech